Accepted Manuscript

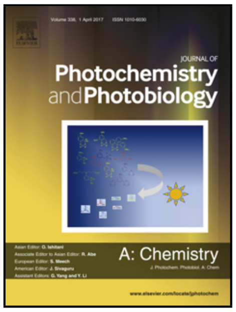

Title: Controlled Photocatalytic Hydrolysis of Nitriles to Amides by Mesoporous MnO_2 Nanoparticles Fabricated by Mixed Surfactant Mediated Approach

Author: Akansha Mehta Soumen Basu

PII: S1010-6030(17)30222-8
DOI: http://dx.doi.org/doi:10.1016/j.jphotochem.2017.04.013
Reference: JPC 10602

To appear in: *Journal of Photochemistry and Photobiology A: Chemistry*

Received date: 21-2-2017
Revised date: 7-4-2017
Accepted date: 11-4-2017

Please cite this article as: A. Mehta, S. Basu, Controlled Photocatalytic Hydrolysis of Nitriles to Amides by Mesoporous MnO_2 Nanoparticles Fabricated by Mixed Surfactant Mediated Approach, *Journal of Photochemistry and Photobiology A: Chemistry* (2017), http://dx.doi.org/10.1016/j.jphotochem.2017.04.013

Controlled Photocatalytic Hydrolysis of Nitriles to Amides by Mesoporous MnO_2 Nanoparticles Fabricated by Mixed Surfactant Mediated Approach

Akansha Mehta and Soumen Basu*

School of Chemistry and Biochemistry, Thapar University, Patiala-147004, India

*Corresponding author. E-mail address: soumen.basu@thapar.edu

Graphical Abstract

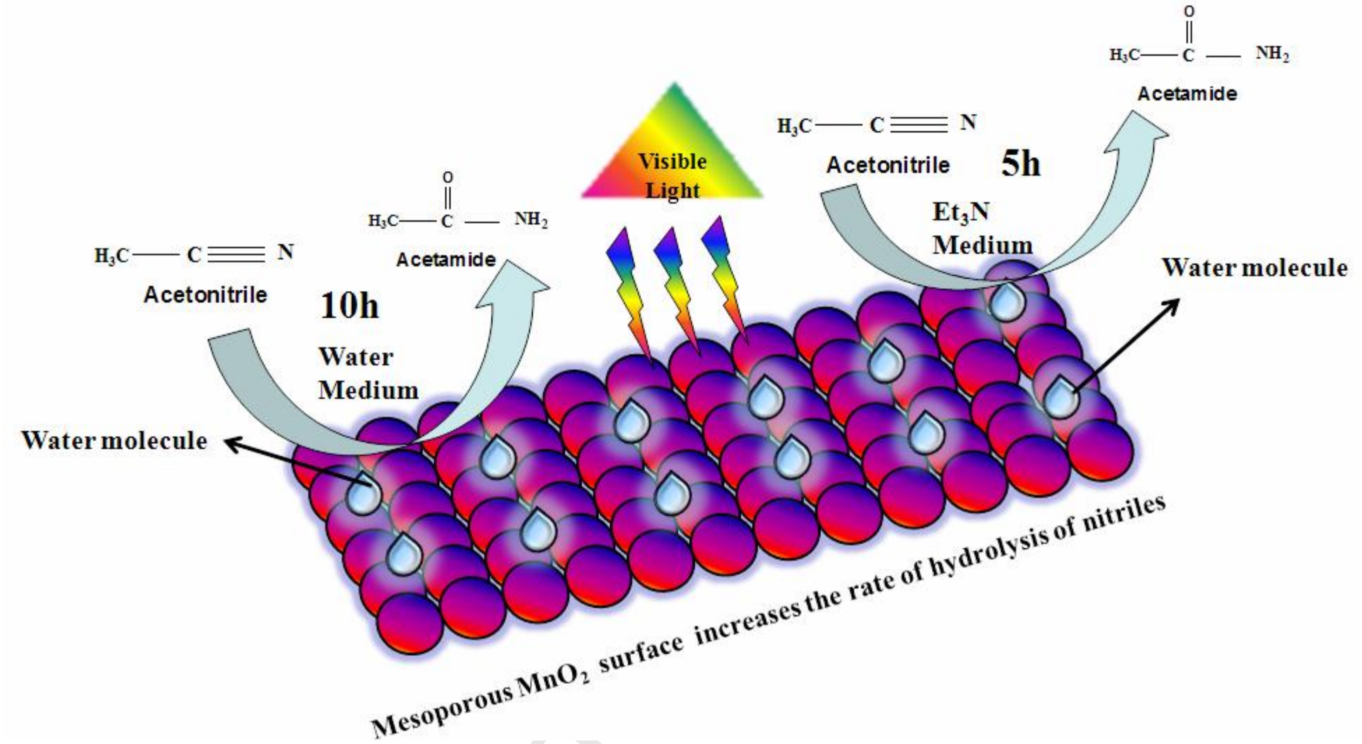

Highlights

- ✓ Synthesis of mesoporous MnO_2 by using mixture of cationic and anionic surfactants with variable pore volume.
- ✓ The cat-anionic surfactant yields 5 times higher surface area ($195.32 m^2/g$) than their corresponding individual form (CTAB 29 m^2/g and SDS 36 m^2/g).
- ✓ Synergic effect, low critical aggregation concentration of cat-anionic surfactant is endorsed for its high surface area.
- ✓ The mesoporous MnO_2 as a novel catalyst for the hydrolysis of nitriles to amides.
- ✓ Higher yield (90%) in basic reaction medium compare to neutral medium (70%).

Abstract

The solid-phase MnO_2 nanoparticles fabricated by surfactant template method were exploited as the photocatalyst for the effective one-step synthesis of amides. Cationic or anionic surfactants and their combinations were used as porous templates to obtain the mesoporous MnO_2 nanoparticles with variable pore volume (0.23 to 1.95 cm^3/g). The morphological and structural observation of the material confirms the uniform facet structure (37.68 nm) of MnO_2 nanoparticles. The surface elemental state was confirmed by XPS analysis confirming Mn $2p_{3/2}$ (642.5 eV) and Mn$2p_{1/2}$ (654.7 eV) spin states, that are common for the tetravalent Mn ions. Presence of surfactant as stabilizer was also witnessed with a strong peak of C 1s (283-286 eV). The textural parameters obtained from XRD and Raman analysis depicted the β-phase and rutile type framework of MnO_2.The selective conversion of nitriles to amides was studied without any acid by products under visible light irradiation in the basic/neutral medium. Amides were obtained from various substrates (nitriles) with excellent yields (70-90%).

Keywords: MnO_2 nanoparticles; synergistic effect of CTAB and SDS; photocatalysis; hydrolysis of nitriles;

1. Introduction

One of the most important industrial reactions in the organic chemistry is amide bond formation as it constitutes important moieties in many pharmaceutical and biologically active ingredients[1]. Moreover, the flattering properties of amides like stability, conformational diversity and high polarity make it one of the most reliable and accepted functional groups in every branch of organic chemistry. Among all the methods reported for the fabrication of amides, hydration of nitriles has become one of the most widely used methods to obtain primary amides. But this is a challenging reaction as there is possibility of acid formation from amides. The hydrolysis reaction is catalysed in acidic and basic medium, but many of the methods requires harsh conditions with poor yields due to further conversion of amides to acids[2, 3]. Improved methods for the selective and controlled synthesis of amides using catalysts under stable conditions are of great demand [4(a)]. In this regard formation of amides by hydrolysis of nitriles using transition metal oxides nanomaterials as a photocatalyst is good choice to obtain better yields. It is a principal objective of the present study to provide a new method for converting nitriles to amides.

Nanoporous transition metal oxides with controlled morphology, porous structures, tunable nano pores and well ordered mesostructures make them ideal photocatalysts in the field of catalysis. During recent times, of all the transition metal oxides, manganese dioxide (MnO_2) nanostructures have received keen attention due to its attractive physical and chemical properties[4(b, c)]. The MnO_2 is non-stoichiometric compound and can exist in different crystallographic forms. The crystallographic forms are generally supposed to be responsible for their variable properties and the controlled synthesis of MnO_2 which make the controlled design of a specific forma primary objective [5]. Previously, many processes have been developed for the synthesis of MnO_2 nanoparticles with different shapes and morphology. Out of all the processes MnO_2 nanostructures are commonly synthesized using hydrothermal treatment[6, 7], sol-gel process[8, 9], refluxing[10, 11] and normal thermal approach[12] for enormous catalytic application [13, 14] because of their different morphology and variable oxidation states. Several attempts have been made to further improve the catalytic activity by using some facile techniques [15, 16] but enhancing surface area is an excellent way to improve its catalytic properties. As a remedial surfactants based synthesis are considered as best route to develop a mesoporous structure. They have the exceptional property to self-organize in the solution, which may modify the interfacial properties and increase the compatibility among the particles. Materials prepared without using surfactants or other stabilizing agents lead to agglomeration as well as reduce the processing temperature of metal oxide and several other materials [17]. Earlier Yan *et al*. have reported the synthesis of MnO_2 using the cationic surfactant (CTAB or CTAC) by direct electrodeposition method with a specific surface area of 102 m^2/g [18], Roy *et al*. have synthesized mesoporous manganese oxides nanostructures by using a bi-template approach with the surface area of 65 m^2/g [19], Zhi *et al.* have fabricated MnO_2 nanoarrays using vacuum assisted nanocasting with a surface area of 139 m^2/g [20], Saputra *et al.* have synthesized one-dimensional MnO_2 nanoparticles with a surface area of 194 m^2/g [21]. But still the role of individual surfactants as a porous template for the synthesis of high surface area mesoporous MnO_2 nanoparticles and their effect to convert nitriles to amides has not been fully explored.

In this regard current work signifies the single step selective and controlled hydrolysis of nitriles to amides under visible light both in the basic and neutral medium using MnO_2 as photocatalyst. The mechanism for the selective fabrication of amides without any acid moieties has also been fully explored.

2. Experimental

2.1 Chemicals and Reagents

Manganese (II) nitrate tetrahydrate ($MnNO_3.4H_2O$), Cetyl trimethylammonium bromide (CTAB), Sodium dodecyl sulphate (SDS) and acetonitrile were received from Aldrich. An aqueous solution of $MnNO_3.4H_2O$ (1 M) with the mixture of CTAB (0.25×10^{-3} M) and SDS (0.25×10^{-3} M) was stirred at normal room temperature. For complete conversion of Mn (II) to Mn (IV), the solution was stirred for 20 min in the presence of NaOH and change in the color of solution was observed from light pink to dark brown, which indicates the formation of MnO_2 nanoparticles denoted as m-MnO_2 (CTAB+SDS) as shown in Fig. S1. The product was recovered by filtration, washing with distilled water, drying and calcined at 623 K for 3 h and used as a solid catalyst for the hydrolysis of nitriles. Similarly, other samples of MnO_2 were also prepared using cationic, CTAB (0.25×10^{-3} M) as well as anionic, SDS (0.25×10^{-3} M) surfactant were denoted as c-MnO_2 and s-MnO_2 respectively.

2.2 Photocatalytic Activity

The photocatalytic experiment was carried out in a test tube containing 5 mL of nitrile in 100 μL of solvent (Et_3N or water) and 20 mg of the catalyst. The reaction mixture was illuminated under visible light (40 W CFL lamp) for 5 h by keeping a distance of 1cm apart from the surface of reaction mixture in the test tube. The reactions was also performed under dark and without catalysts but no conversion of nitriles to amides are obtained which confirms that reaction does take place without the presence of both visible light and catalyst. The product was isolated from the reaction mixture by using nylon syringe filter (0.22μm) and the product was quantitatively analysed by GC-MS and ^{13}C NMR to confirm the formation of amides.

3. Results and Discussion

3.1 Characterization of Photocatalyst

The phase identification of crystalline MnO_2 was analyzed through XRD analysis (PANALYTICAL X'Pert PRO) with Cu Kα (λ=1.540 Å) as radiation source over the range 0°≤2θ≤90°.The diffraction pattern of as- synthesized different MnO_2 samples exhibits intense diffraction peaks of (110), (101), (211), (220) and (002) which is characteristics of β-MnO_2 structure (JCPDS Card no. 24-0735) with lattice parameters a = 4.399 Å, c = 2.874 Å and space group $P4_2/mnm$ (Fig. 1a).Some other peaks are also highlighted in the Fig. 1 which are due to an addition of surfactants. The crystallite size and lattice strain was calculated by Scherrer equation ($D = 0.9\lambda/\beta\cos\theta$), the sample m-$MnO_2$ has largest crystallite size and smallest lattice strain (13nm, 0.0129) compared to c-MnO_2 and s-MnO_2, which is shown in Table 1. This larger crystallite size is due to self- assembly in cat-anionic surfactant, which occurs synergistically because of electrostatic attraction between the polar head groups of the surfactants.

The chemical composition of m-MnO_2 sample was studied by X-ray photoelectron spectroscopy (XPS) shown in Fig. 2, the survey spectra reveals the presence of elements like Mn, O, C. The peaks for β-MnO_2 corresponding to Mn $2p_{3/2}$ and Mn $2p_{1/2}$ were observed at a binding energy of 642.5 and 654.7 eV respectively, which clearly indicates the presence of tetravalent Mn ions. Similarly the deconvulated peaks of O 1s at 528.7 eV and 531.3 eV are due to the linkage of Mn-O and Mn-OH respectively. The C 1s peaks at 283.9 eV and 286.2 eV are associated with the presence of surfactant. The symmetric stretching vibration (Mn-O) of $[MnO_6]$ groups is analyzed by Raman spectra (Fig. S2 in supporting information). The sharp peaks were observed at 310 cm^{-1},475 cm^{-1}, 537 cm^{-1} and 662 cm^{-1} are indicative of a well-developed rutile type framework of MnO_2 [22].

The morphology and surface characteristics were confirmed by FESEM (JEOL JSM-6510LV) and HRTEM (FEI Technai G2 F20 operating at 200KV) studies. The FESEM studies (Fig.S3) displayed the discrete morphology of the m-MnO_2 and the mean particle size distribution calculated by TEM analysis has been observed to be of 30-40 nm (Fig. 3(d)), measured by Axio Vision Rel. 4.9.1.0 software. The HRTEM images explore faceted morphology with little aggregating nature, which may be due to the drying of the sample on the TEM grid. Fig. 3(d) also shows the plot of the frequency of particles against the logarithm of size. The particle size follows the following lognormal distribution function;

$$f(d) \; = \frac{1}{\sqrt{2\pi}.\sigma.d_i} e^{-\left(\frac{(log(d_i)-\mu)^2}{2\sigma^2}\right)}$$

$$\text{where } \mu = \frac{\sum log(d_i)}{\sum n_i};\text{and } \sigma = \sqrt{\frac{\sum(log(d_i)-\mu)^2}{\sum n_i}}$$

Where *f (d)* designates the lognormal distribution of particle size, d_i represents the size of an i^{th} particle of NbC, $\sum n_i$ is the total number of particles in consideration, μ is mean diameter and σ is the standard deviation of particle size. The variation in average particle size calculated by different criteria is due to the few agglomerated nanoparticles. The structure, dispersion and lattice fringes of MnO_2 nanoparticles are shown in HRTEM micrograph (Fig. 2) which corresponds to (101) plane with interplanar distance of 0.39-0.80 nm that was further supported by the SAED pattern (Fig. 3 Inset). The energy dispersive analysis (EDX) also confirmed the purity of the MnO_2 nanoparticles (Fig. S4).

The N_2 adsorption- desorption isotherms and pore size distribution plot (Table 1) was monitored with the help of BEL mini-II, Micro Trac Corp. Pvt. Ltd, Japan. The adsorption results exhibit type IV classification which presents their mesoporous characteristics (Fig. 4). The m-MnO_2 shows highest surface area (195.3 m^2/g) and smaller pore diameter (40.48 nm: Fig S4) due to the charges present on the surface of surfactants as well as on metal ions (positive charge) [23].

3.2 Mechanism for the Synthesis of Mesoporous MnO_2

Mixed micelle formation in aqueous phase is usually achieved when two surfactants of the different polarities are mixed. The hydrophilic polar head of cat-anionic surfactants were actively participating in the reaction which facilitates by either the electrostatic attraction or repulsion between the ions. Generally, rod-shaped micelles are formed in the case of CTAB rich corner and spherical micelles are formed in SDS rich corner. The morphology suddenly turned upon addition of equal amount of SDS into CTAB results in wormlike micelles because SDS reduces the surface potential by charge neutralization and also increment in the ionic strength is observed by an asset of the released counter ions. Thus, oppositely charged cat-anionic surfactants shows enrichment in a synergistic effect over that of either parent surfactant, an effect which may be exploited in various catalytic applications[24].

3.2 Photocatalytic Activity

The aim of present work is to study the reactivity of m-MnO_2 by converting nitriles into amides under visible light in the weakly basic medium as well as in neutral medium. The product was isolated from the reaction mixture and characterized by GC-MS and ^{13}C NMR (Fig. 5 (a)) to confirm the formation of amides. The photocatalytic activity is analyzed by using all three photocatalysts (c-MnO_2, s-MnO_2, m-MnO_2).The yield calculated from c-MnO_2 and s-MnO_2 is around 50 % which is very less as compare to m-MnO_2 (70 - 90 %). The GC-MS spectra of the product authenticate the formation of amides from the reaction of acetonitrile. The fragmentation pattern shows, peak at m/z = 59 due to acetamide (Fig. 5(b)). The ^{13}C NMR spectrum shows carbonyl carbon peak at δ = 171.67 ppm and the methyl carbon peak at 22.72 ppm which authenticates the formation of acetamide (Fig. 5(a)). A similar strategy was followed for propionitrile and acrylonitrile compounds moreover the product was analyzed by GC-MS (Fig. S6, S7). The % yield and reaction time for all the nitriles are summarized in Table 2. The other importance of the catalyst is its reusability, which remains constant (Fig. S5) even after 5 cycles. The photocatalyst is easily separable from the reaction mixture by centrifugation process and has no permanent adsorption of nitriles/amides over the catalyst. The % yield of the catalyst is calculated theoretically (Actual yield/theoretical yield*100) which lies in the range of 70-90 % as presented in Table 2.

The reported mechanism suggests that the reaction of hydrolysis of nitriles took place in two steps [25]. The first step is conversion of acetonitrile to acetamide and second step is rapid hydrolysis to acetic acid. But, the brightness of m-MnO_2 catalyst falls on this point that it limits the reaction up to the formation of acetamide giving desired product. This happens because MnO_2 confines the water molecule droplets and there is no direct hydration of amides. (hydration directly in the presence of water can undergo further hydrolysis to the acid) [26,27]. The catalytic activity of m-MnO_2 is attributed to its large surface area along with additional active sites which is pictorially represented in Fig. 7. The proposed mechanism for the hydrolysis of nitriles to amides in a basic/neutral medium under visible light is heterogeneously catalyzed hydrolysis involving water on the surface of the catalyst, as m-MnO_2 retains moisture on its surface. The reaction of nitriles only with water (neutral medium) would be so slow (10 h) because of the poor nucleophilic nature of water and results in fewer yields (70-80 %). So, the reaction is carried out in alkaline medium (base catalyzed reaction) to activate the nitrile group in a short period of time to get good yields (80 - 90 %) (Fig. 7). The reaction strategy for the synthesis of m-MnO_2 is quite simple, cost effective and is devoid of any harsh atmospheric conditions. By observing several advantages in the present strategy it can be mentioned that commercially available MnO_2 and other reported MnO_2 catalysts could not produce such effective products with good yields under the same protocol [28, 29].

Conclusion

A pioneering synthetic approach is designed for the conversion of nitriles to amides with excellent yields. The mechanism of the hydrolysis reaction under visible light is also explored which shows that reaction of nitriles only with water (neutral medium) is slow due to poor nucleophilic nature of water and gives fewer yields as compare to basic medium. Cationic, anionic and cat-anionic surfactants were used as template for controlling the shape; size and surface area of catalysts. The hydrophilic polar head of both cat-anionic surfactants were found to participate actively by either electrostatic attraction or repulsion between ions which leads to its higher synergistic effect and catalytic activity. Different oxidation states and structural parameters of the m-MnO_2 were confirmed by Raman and XPS studies. The morphology and textural properties were discussed to determine the particle size and pore composition of the catalyst. The present protocol is relevant for the selective formation of amides thus have high potential application for the hydrolysis of different organic compounds.

Conflict of interests:

The authors declare that there is no conflict of interests regarding the publication of this.

Acknowledgements

Authors are thankful to DST (Grant No: SB/FT/CS-178/2013), New Delhi, BRNS (Grant No: 34/14/63/2014) for financial assistance and Dr. S. K. Pandey, School of Chemistry & Biochemistry, Thapar University for discussion and suggestions.

References

[1] H.C. Kolb, M.G. Finn, K.B. Sharpless. Angew. Chem. Int. Edit. 40(2001) 2004-2021.

[2] F. Nawaz, Y. Xie, H. Cao, J. Xiao, X. Zhang, M. Li, F. Duan. Catal. Today 258 (2015) 595-601.

[3] R.-S. Luo, X.-A. Mao, Z.-Q. Pan, Q.-H. Luo. Spectrochim. Acta Part A: Mol. Biomol. Spectrosc. 56 (2000) 1675-1680.

[4] (a) V.R. Pattabiraman, J.W. Bode. Nature 480 (2011) 471-479.

(b) S. R. Ede, S. Anantharaj, U. Nithiyanantham, S. Kundu, Phys. Chem. Chem. Phys. 17 (2015) 5474-5484.

(c) S. R. Ede, A. Ramadoss, S. Anantharaj, U. Nithiyanantham, S. Kundu, Phys. Chem. Chem. Phys. 16 (2014) 21846-21859.

[5] F. Xu, T. Wang, W. Li, Z. Jiang. Chem. Phys. Lett. 375 (2003) 247-251.

[6] A.G. da Silva, C.M. Kisukuri, T.S. Rodrigues, E.G. Candido, I.C. de Freitas, A.H. da Silva, J.M. Assaf, D.C. Oliveira, L.H. Andrade, P.H. Camargo. Appl. Catal. B: Environ. 184 (2016) 35-43.

[7] G. Qiu, H. Huang, S. Dharmarathna, E. Benbow, L. Stafford, S.L. Suib. Chem. Mater. 23 (2011) 3892-3901.

[8] X. Wang, A. Yuan, Y. Wang. J. of Power Sources 172 (2007) 1007-1011.

[9] J. Lin, M. Yu, C. Lin, X. Liu. J. Phys. Chem. C 111 (2007) 5835-5845.

[10] J. Yan, Z. Fan, T. Wei, W. Qian, M. Zhang, F. Wei. Carbon 48 (2010) 3825-3833.

[11] Y. Lei, J. Li, Y. Wang, L. Gu, Y. Chang, H. Yuan, D. Xiao. ACS Appl. Mater. Inter. 6 (2014) 1773-1780.

[12] Y. Muraoka, H. Chiba, T. Atou, M. Kikuchi, K. Hiraga, Y. Syono, S. Sugiyama, S. Yamamoto, J.-C. Grenier. J. Solid State Chem. 144 (1999) 136-142.

[13] X. Xu, X. Zhou, X. Li, F. Yang, B. Jin, T. Xu, M. Li. Mater. Res. Bull. 59 (2014) 32-36.

[14] G. Cheng, L. Yu, B. Lan, M. Sun, T. Lin, Z. Fu, B. Xu. Mater. Res. Bull. 75 (2016) 17-24.

[15] T. Lin, L. Yu, M. Sun, G. Cheng, B. Lan, Z. Fu. Chem. Eng. J. 286 (2016) 114-121.

[16] L. Li, C. Nan, J. Lu, Q. Peng, Y. Li. Chem. Commun. 48 (2012) 6945-6947.

[17] T. Hyeon, S.S. Lee, J. Park, Y. Chung, H.B. Na. J. Am. Chem. Soc. 123 (2001) 12798-12801.

[18] Y. Li, X. Cai, W. Shen. Electrochim. Acta 149 (2014) 306-315.

[19] M.K. Naskar, M. Roy. Phys. Chem. Chem. Phys. 18 (2016) 5253-5263.

[20] B. Zhi, H. Ding, D. Wang, Y. Cao, Y. Zhang, X. Wang, Y. Liu, Q. Huo. J. Mater. Chem. A 2 (2014) 2374-2382.

[21] E. Saputra, S. Muhammad, H. Sun, H.M. Ang, M. Tade, S. Wang. Environ. Sci. Tecnol. 47 (2013) 5882-5887.

[22] T. Gao, H. Fjellvåg, P. Norby. Anal. Chim. Acta 648 (2009) 235-239.

[23] S.R. Raghavan, G. Fritz, E.W. Kaler. Langmuir 18 (2002) 3797-3803.

[24] (a) R.D. Koehler, S.R. Raghavan, E.W. Kaler. J. Phys. Chem. B 104 (2000) 11035-11044.

(b) M. S. Bakshi, Cryst. Growth Des. 16 (2015) 1104-1133.

[25] J. Ma, X. Zhang, N. Zhao, F. Xiao, W. Wei, Y. Sun, Theochem. 911 (2009) 40-45.

[26] J.N. Moorthy, N. Singhal. J. Org. Chem. 70 (2005) 1926-1929.

[27] E. Cariati, C. Dragonetti, L. Manassero, D. Roberto, F. Tessore, E. Lucenti. J. Mol. Catal. A: Chem. 204 (2003) 279-285.

[28] S. Jana, S. Praharaj, S. Panigrahi, S. Basu, S. Pande, C.-H. Chang, T. Pal. Org. Lett. 9 (2007) 2191-2193.

[29] S. Jana, S. Basu, S. Pande, S.K. Ghosh, T. Pal. J. Phys. Chem C 111 (2007) 16272-16277.

Figures

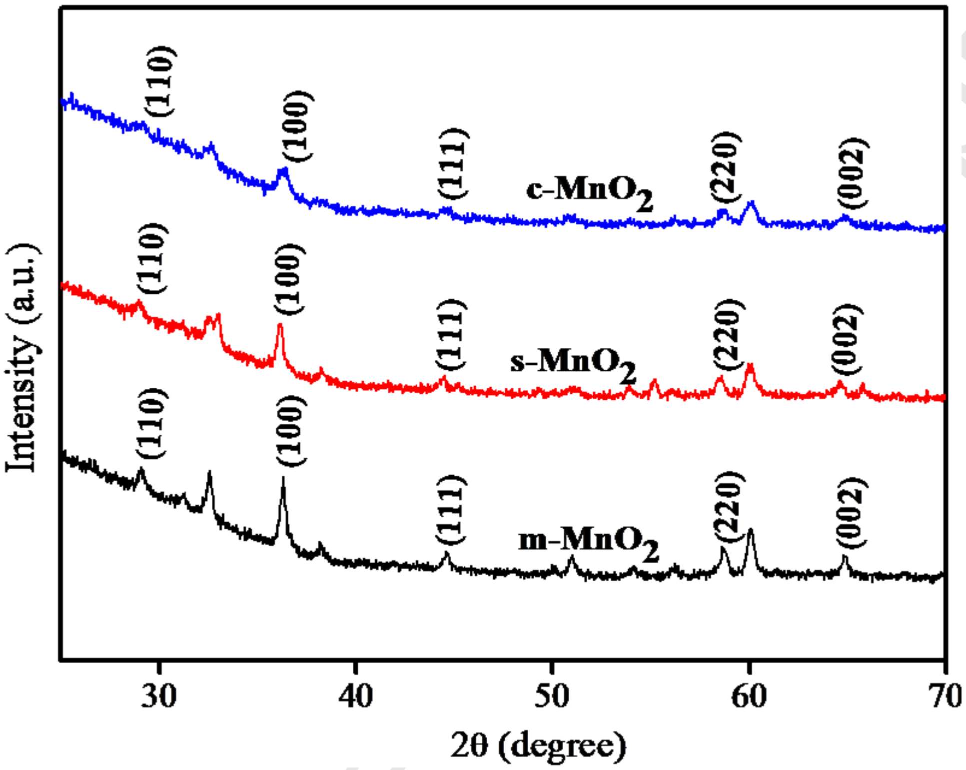

Fig. 1: XRD pattern for different MnO_2 nanostructures.

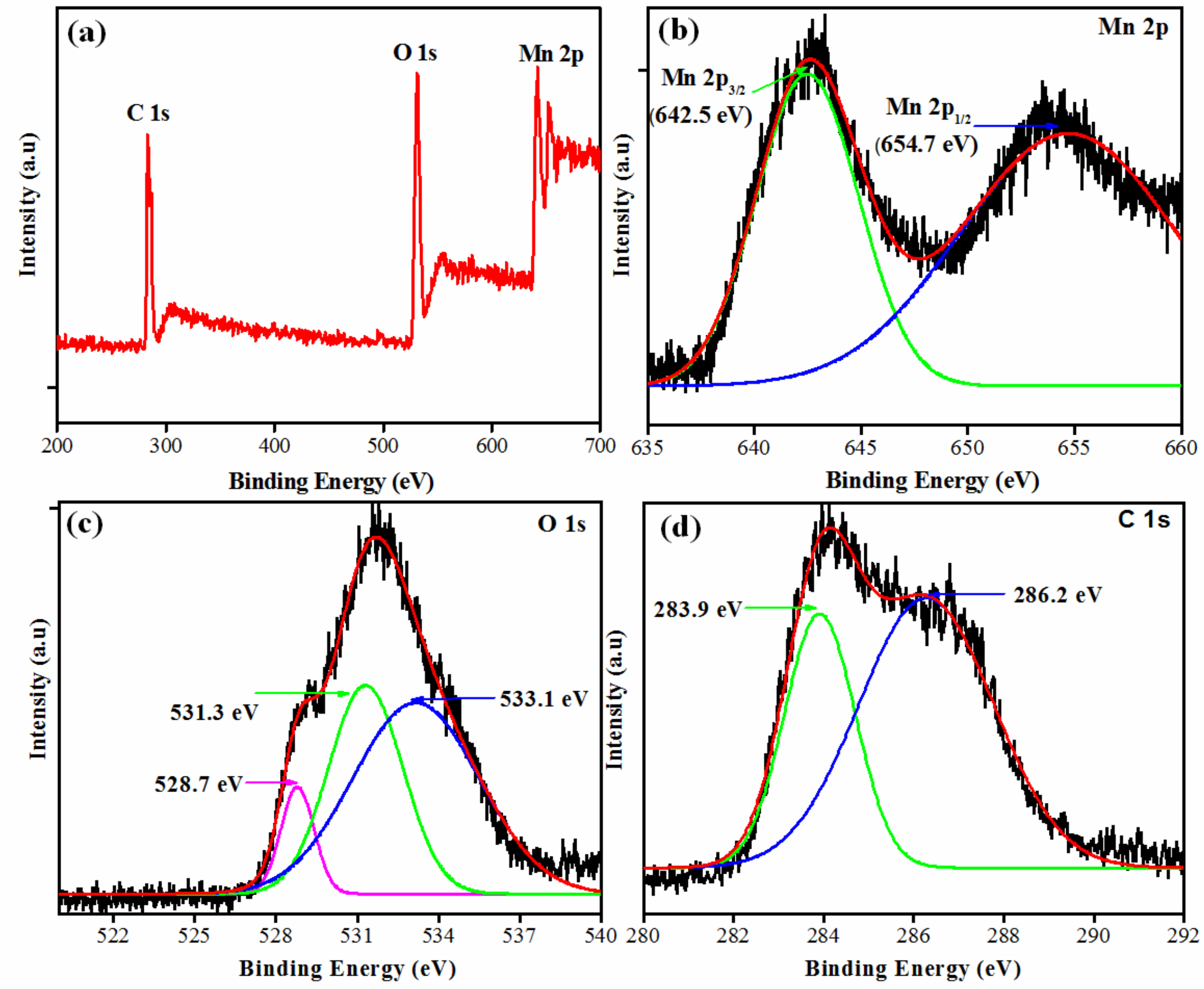

Fig. 2: XPS spectrum of m-MnO_2.

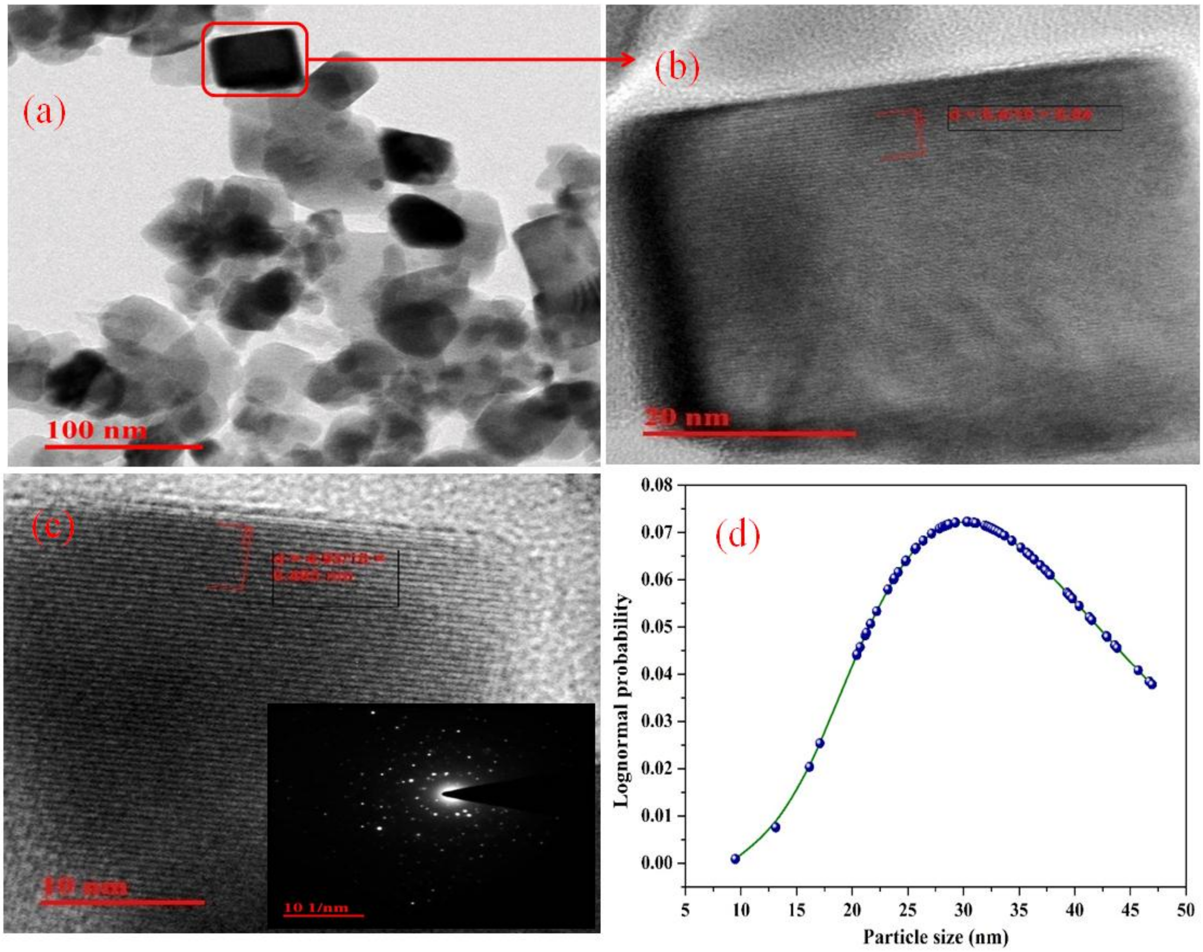

Fig. 3: HRTEM images with particle size distribution plot and SAED pattern of m-MnO_2.

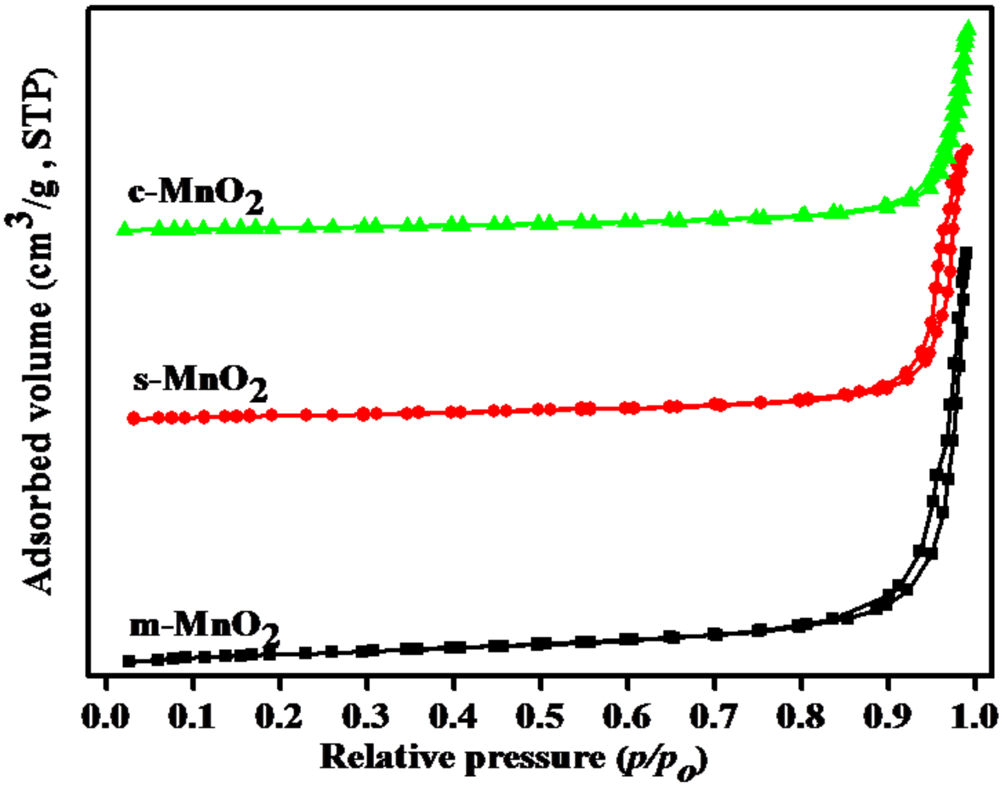

Fig. 4: N_2 adsorption-desorption isotherms for MnO_2 nanostructures synthesized by using CTAB (c-MnO_2), SDS (s-MnO_2) and CTAB+SDS (m-MnO_2).

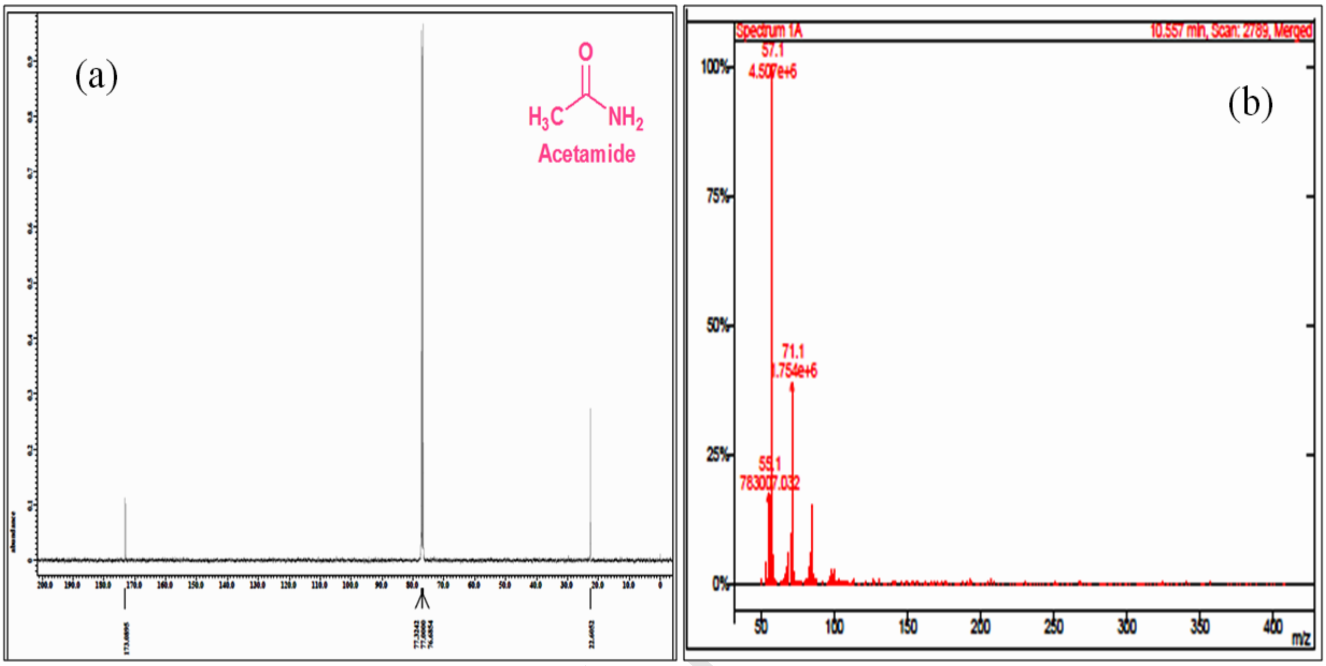

Fig. 5: (a) ^{13}**C**-NMR spectrum of isolated acetamide in $CDCl_3$, **(b)** GC-MS spectra of the product (acetamide, as the fragmentation pattern shows peak at m/z 59 due to acetamide).

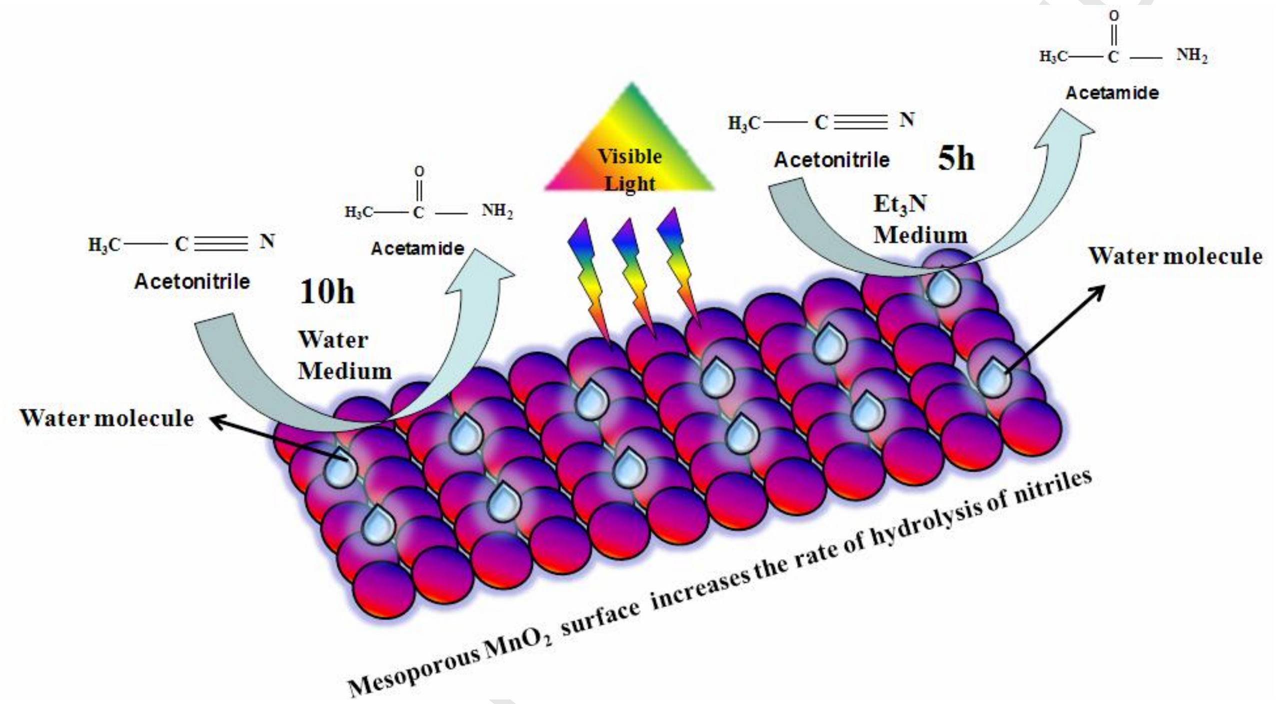

Fig. 6: Pictorial representation of the hydrolysis of acetonitrile to acetamide in basic/neutral medium.

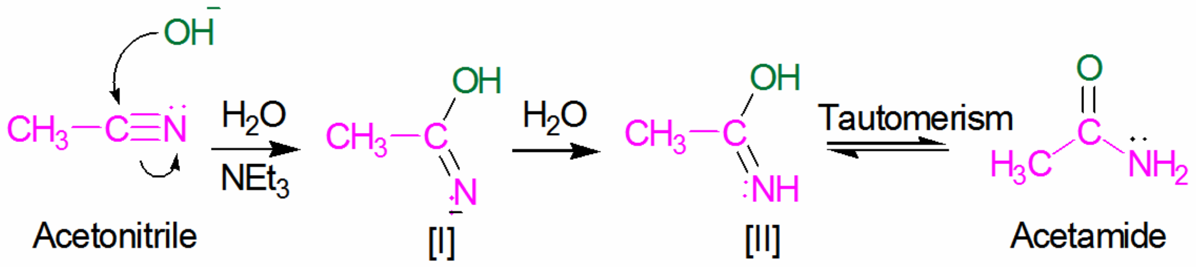

In 1st step the MnO2 which is acting as a catalyst provides water molecule with triethylamine to form transition state [I].
In 2nd step another water molecule provides proton to form intermediate state [II].
In 3rd step intermediate state [II] tautomerise to form acetamide.

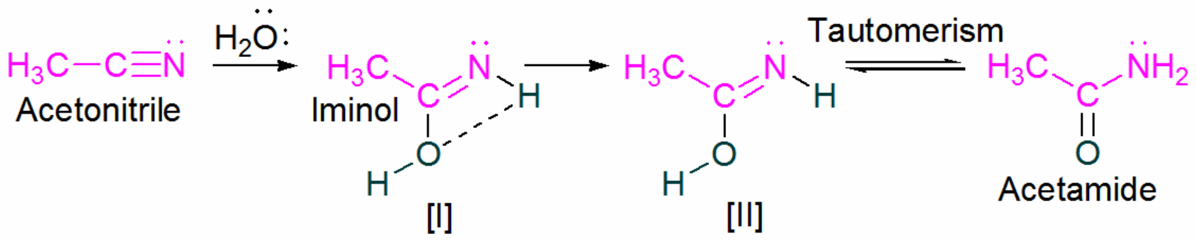

In 1st step the water molecule performs a nucleophilic attack on the nitrile carbon, concerted with the transfer of a proton to the nitrile nitrogen forming an transition state [I].
In 2nd step the protons on [I] have to flip to allow for the next step of the reaction, but such flipping can be assumed to occur very fast to give intermediate state [II].
In 3rd step the intermediate state [II] then tautomerize to give final products i e. amide.

Fig. 7: Proposed reaction mechanism for the hydrolysis of nitriles to amides in neutral/basic medium.

Table 1. Textural properties of different MnO_2 nanostructures.

Samples	**d^a**	**$\varepsilon_L{}^b$**	**$S_{bet}{}^c$ (m^2g)**	**$V_p{}^d$ (Cm^3/g)**	**$D_{BJH}{}^e$**
CTAB	**9.28**	**0.0126**	**29.0**	**0.23**	**46.79**
SDS	**9.09**	**0.0129**	**36.0**	**0.30**	**46.85**
CTAB+SDS	**13**	**0.0090**	**195.3**	**1.95**	**40.48**

[a] Crystallite size determined from scherrer formula.

[b] Lattice strain determined from XRD analysis.

[c] BET surface area calculated from the linear part of the BET plot ($p/p_0 = 0.05\text{-}0.25$).

[d] Total pore volume, taken from the volume of N_2 adsorbed at $p/p_0 = 0.990$.

[e] Mean pore diameter estimated using the adsorption isotherm.

Table 2. Catalytic activity of m-MnO_2 with different substrates and solvents.

Substrate	Product	Medium	Reaction Time (h)	Yield (%)
 **Acetonitrile**	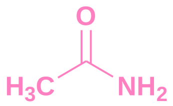 **Acetamide**	Triethylamine	5	90
		Water	10	75
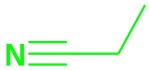 **Propionitrile**	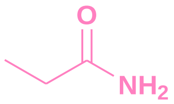 **Propionamide**	Triethylamine	4	88
		Water	8	72
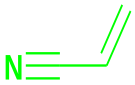 **Acrylonitrile**	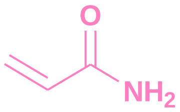 **Acrylamide**	Triethylamine	4	85
		Water	8	71